Received: 16 April 2021 | Revised: 31 May 2021 | Accepted: 13 June 2021

DOI: 10.1002/aoc.6348

RESEARCH ARTICLE

Applied Organometallic Chemistry WILEY

Palladium complexes derived from benzoylthiourea ligands: Synthesis, crystal structure, and catalytic application in Suzuki C–C coupling reactions

Ummuhan Solmaz[1] | **Ilkay Gumus**[2,3] | **Mustafa Kemal Yilmaz**[1] | **Simay Ince**[2] | **Hakan Arslan**[1]

[1]Department of Chemistry, Faculty of Arts and Science, Mersin University, Mersin, Turkey

[2]Department of Nanotechnology and Advanced Materials, Institute of Science, Mersin University, Mersin, Turkey

[3]Department of Basic Sciences, Faculty of Maritime, Mersin University, Mersin, Turkey

Correspondence
Hakan Arslan, Department of Chemistry, Faculty of Arts and Science, Mersin University, Mersin 33343, Turkey.
Email: hakan.arslan@mersin.edu.tr

Funding information
Mersin University Research Fund, Grant/Award Number: 2018-3-AP4-3090

Abstract

$[PdCl_2(HL^1\text{-}\kappa S)_2]$ and $[PdCl_2(HL^2\text{-}\kappa S)_2]$ complexes were formed from neutral monodentate modes of HL^1 and HL^2 ligands, which are coordinated to the palladium(II) center, respectively. $[Pd(L^1\text{-}\kappa^2S,O)_2]$ and $[Pd(L^2\text{-}\kappa^2S,O)_2]$ complexes were obtained by recrystallization of corresponding $[PdCl_2(HL^1\text{-}\kappa S)_2]$ and $[PdCl_2(HL^2\text{-}\kappa S)_2]$ complexes as anionic bidentate coordination modes. All palladium(II) complexes were characterized by elemental analysis, FT-IR, and NMR (^1H and ^{13}C) techniques. The molecular structure of $[Pd(L^1\text{-}\kappa^2S,O)_2]$ and $[Pd(L^2\text{-}\kappa^2S,O)_2]$ was also confirmed by single-crystal X-ray diffraction method. The roles and behaviors of the prepared four palladium(II) complexes in catalytic investigations for the Suzuki C–C coupling reaction were examined for the first time. The complexes acted as the excellent catalyst precursor and showed highly catalytic activity for the Suzuki C–C coupling reaction of various arylhalides with phenylboronic acid at low catalyst loading (0.01 mol%).

Highlights

- All compounds were structurally characterized by FT-IR, ^1H NMR, and ^{13}C NMR spectroscopies.
- $[Pd(L\text{-}\kappa^2O,S)_2]$ complex was obtained by recrystallization of $[PdCl_2(HL\text{-}\kappa S)_2]$ complex.
- The molecular structures of $[Pd(L^1\text{-}\kappa^2S,O)_2]$ and $[Pd(L^2\text{-}\kappa^2S,O)_2]$ complexes were confirmed by X-ray diffraction analysis in single crystal.
- The structure of the compounds was stabilized by hydrogen bond interactions.
- All palladium precursors performed excellent catalytic activity in the Suzuki C–C coupling reaction.

KEYWORDS

benzoylthiourea, catalytic activity, crystal structure, palladium complexes, Suzuki C–C coupling reaction

1 | INTRODUCTION

Palladium metal is considered as a soft metal (Class B) and known with the rich chemical properties. Comprehensive applications of palladium chemistry have been developed with various organic transformations such as Suzuki, Heck, Sonogashira, Corriud–Kumada, Stille, Tsuji–Trost, Ullmann, and Hiyama through the C–C coupling reactions.[1–5] Palladium-catalyzed Suzuki C–C coupling reactions of arylhalides with arylboronic acids have been considered as one of the most valuable synthetic methods for the preparation of symmetric and nonsymmetric biaryl compounds that are widely used in numerous natural products, polymers, agrochemicals, pharmaceuticals, materials, and synthetic chemistry.[6–16] In addition, palladium complexes that can be varied with many ligands, such as phosphines,[17–20] imidazole,[21] pyridine,[22] dibenzylideneacetone,[23] porphyrins,[24] phthalocyanines,[25] and thiols,[26] were successfully carried out as catalyst for this coupling reaction. As compared with benzoylthiourea ligands, some of the ligands are relatively more expensive, less thermally and chemically stable.[27–37] Moreover, more amounts of catalyst or longer time may be required for catalytic conversions.[22,38,39] On the other hand, benzoylthiourea ligands are generally stable in air and moisture, and their catalytic properties can be easily controlled by changing the *N*-substitution.[34,37,40,41] Moreover, *N*-substituted benzoylthioureas are the organic compounds with donor atoms that provide a large number of bonding possibilities such as nitrogen, sulfur, and oxygen atoms.[30,42,43] Thus, these ligands can be coordinated with various transition metals or ions as neutral monodentate[44] or anionic bidentate coordination modes.[45,46] Although these ligands exhibit common anionic O,S-bidentate coordination modes, the unusual neutral monodentate coordination through only sulfur atoms is reported in some studies.[44,47,48] In the catalytic reactions and other organic transformations, there are a number of applications of benzoylthiourea-derived compounds due to their different coordination modes. The benzoylthiourea ligands have only been applied in the Sonogashira coupling reactions, and also there has been no report on the Suzuki C–C coupling reaction so far.[30] Therefore, in this study, we wanted to apply benzoylthiourea-palladium(II) complexes as catalysts in the Suzuki C–C coupling reactions, and we found that these ligand systems were very active, robust, and suitable for the formation of biaryl units with very low catalyst loading. Besides, the different coordination modes of these ligands were also investigated by using X-ray diffraction analysis.

2 | EXPERIMENTAL

2.1 | Instrumentation

^{1}H and ^{13}C NMR spectra were obtained on a Bruker Avance III 400 MHz Ultrashield Plus Biospin spectrometer. The deuterated solvent $CDCl_3$ was used as purchased. FT-IR spectra were recorded on a PerkinElmer Spectrum 100 series FT-IR spectrometer (4000–400 cm^{-1}; number of scans: 250; resolution: 1 cm^{-1}) and were reported in cm^{-1} units. Carbon, hydrogen, and nitrogen analyses were carried out on a Carlo Erba MOD 1106 elemental analyzer.

The X-ray single-crystal diffraction data were recorded on a Bruker APEX II CCD diffractometer. A suitable crystal was selected and coated with Paratone oil and mounted onto a Nylon loop on a Bruker APEX II CCD diffractometer. The crystal was kept at T = 100 K during the collection of the data. The data were collected with CuKα (λ = 1.54178 Å) radiation for $[Pd(L^1\text{-}\kappa^2S,O)_2]$ and MoKα (λ = 0.71073 Å) radiation for $[Pd(L^2\text{-}\kappa^2S,O)_2]$ at a crystal-to-detector distance of 40 mm. Using Olex2,[49] the structure was solved with the Superflip[50–52] structure solution program using the charge flipping solution method and refined by full-matrix least-squares technique on F^2 using ShelXL[53] with refinement of F^2 against all reflections. Hydrogen atoms were constrained by different maps and were refined isotropically; in addition, all non-hydrogen atoms were refined anisotropically. The molecular structure plots were prepared using PLATON or Olex2.[49–54]

Gas chromatography (GC) analyses were carried out on a Shimadzu GC-2010 Plus series gas chromatograph equipped with a 30 m × 0.25 mm × 0.25 μm film thickness Rxi-5ms (5% diphenyl:95% dimethylpolysiloxane) capillary column. Thin layer chromatography (TLC) was monitored on a silica gel plate (Merck Kieselgel 60 F_{254}).

The transmission electron microscopy (TEM) measurement was carried out with a FEI Talos F200S, operated at 200 kV. The particle size and standard deviation were determined by counting 200 particles from enlarged TEM images.

2.2 | Synthesis of ligands

All chemicals used for the preparation of the ligand were purchased from Sigma-Aldrich, and the chemicals were of reagent grade quality. 4-Chloro-*N*-(di-*n*-ethylcarbamothioyl)benzamide (HL^1) and 4-chloro-*N*-(di-*n*-propylcarbamothioyl)benzamide (HL^2) were prepared according to previously published method.[55–58] A solution of 4-chlorobenzoyl chloride (5×10^{-2} mol) in

acetone (50 mL) was added dropwise to a suspension of potassium thiocyanate (5×10^{-2} mol) in acetone (30 mL). The reaction mixture was heated under reflux for 30 min and then cooled to room temperature. A solution of dialkylamine (diethylamine or di-*n*-propylamine) (5×10^{-2} mol) in acetone (10 mL) was added, and the resulting mixture was stirred for 2 h. Hydrochloric acid (0.1 N, 300 mL) was added, and the solution was filtered. The solid product was washed with water and purified by recrystallization from ethanol/dichloromethane mixture (1:1, *v*:*v*) (Scheme 1).

4-Chloro-*N*-(di-ethylcarbamothioyl)benzamide (**HL^1**)

Color: White. Yield: 80% (1.083 g). M.p.: 153–155°C. FT-IR (ATR, ν, cm^{-1}): ν(N-H) 3275 (w); ν (Ar–H) 3056 (w); ν(C–H) 2978, 2933, 2875 (w); ν(C=O) 1675 (s); ν(C=S) 1281 (s); ν(C–Cl) 749 (w). ^{1}H NMR (400 MHz, $CDCl_3$, δ, ppm): 8.27 (s, 1H, NH), 7.78 (d, $J = 8.5$ Hz, 2H, Ar–H), 7.45 (d, $J = 8.5$ Hz, 2H, Ar–H), 4.03 (d, $J = 4.8$ Hz, 2H, N–CH_2), 3.59 (d, $J = 7.6$ Hz, 2H, N–CH_2), 1.33 (td, $J = 29.0$, 6.3 Hz, 6H, CH_3). ^{13}C NMR (100 MHz, $CDCl_3$, δ, ppm): 179.1 (C=S), 162.8 (C=O), 139.4, 131.1, 129.2 (C–Ar), 48.1 (C–N), 47.8 (C–N), 13.2 (CH_3), 11.5 (CH_3). Anal. calcd. for $C_{12}H_{15}ClN_2OS$: C, 53.23; H, 5.58; N, 10.35. Found: C, 53.19; H, 5.50; N, 10.25%.

4-Chloro-*N*-(di-*n*-propylcarbamothioyl)benzamide (**HL^2**)

Color: White. Yield: 75% (1.12 g). M.p.: 98–99°C. FT-IR (ATR, ν, cm^{-1}): ν(N–H) 3276, 3212 (w); ν(C–H) 2966, 2933, 2876 (w); ν(C=O) 1690 (s); ν(C=S) 1257 (s); ν(C–Cl) 748.84 (w). ^{1}H NMR (400 MHz, $CDCl_3$, δ, ppm): 8.29 (s, 1H, NH), 7.78 (d, $J = 8.2$ Hz, 2H, Ar–H), 7.45 (d, $J = 8.5$ Hz, 2H, Ar–H), 3.94 (t, $J = 12.8$, 7.4 Hz, 2H, N–CH_2), 3.49 (t, $J = 192.3$, 178.5 Hz, 2H, N–CH_2), 1.88–1.79 (m, 2H, CH_2), 1.76–1.66 (m, 2H, CH_2), 1.02 (t, $J = 7.5$, 0.9 Hz, 3H, CH_3), 0.89 (t, $J = 7.5$, 0.4 Hz, 3H, CH_3). ^{13}C NMR (100 MHz, $CDCl_3$, δ, ppm): 179.8 (C=S), 162.6 (C=O), 139.4, 131.2, 129.2 (C–Ar), 55.1 (C–N), 21.5 (CH_2), 19.8 (CH_2), 11.3 (CH_3). Anal. calcd. for $C_{14}H_{19}ClN_2OS$: C, 56.27; H, 6.41; N, 9.37. Found: C, 56.25; H, 6.39; N, 9.31%.

2.3 | Synthesis of the palladium(II) complexes

2.3.1 | Synthesis of dichloro *bis*[4-chloro-*N*-(di-ethylcarbamothioyl)benzamido-κS] palladium(II) [$PdCl_2$(HL^1-κS)$_2$]

4-Chloro-*N*-(di-ethylcarbamothioyl)benzamide (HL^1) (1.1×10^{-2} mol) dissolved in acetonitrile was added dropwise to an acetonitrile solution of $PdCl_2$ (5×10^{-3} mol) at room temperature. The resulting mixture was stirred overnight. The orange powder that formed was filtered and washed with diethyl ether and then dried in vacuum[59] (Scheme 2).

Color: Orange. Yield: 78%. FT-IR (ATR, ν, cm^{-1}): ν (NH) 3122, 3087 (w); ν (CH) 2961, 2935, 2874 (w);

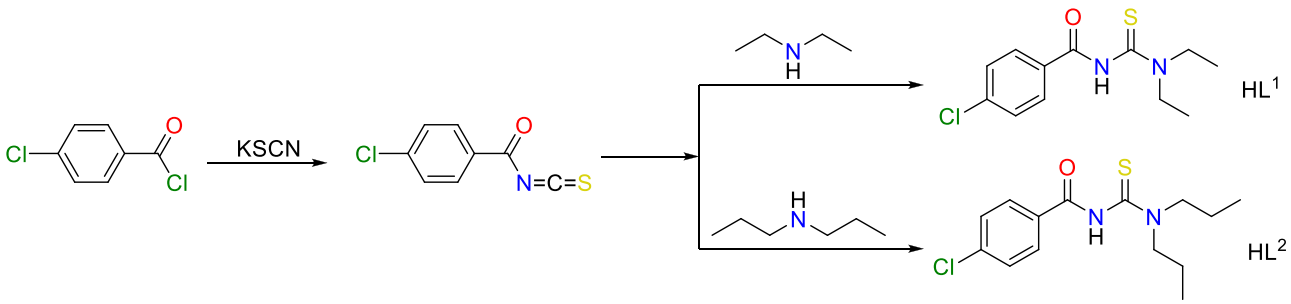

SCHEME 1 Synthesis mechanism of the HL^1 and HL^2 ligands

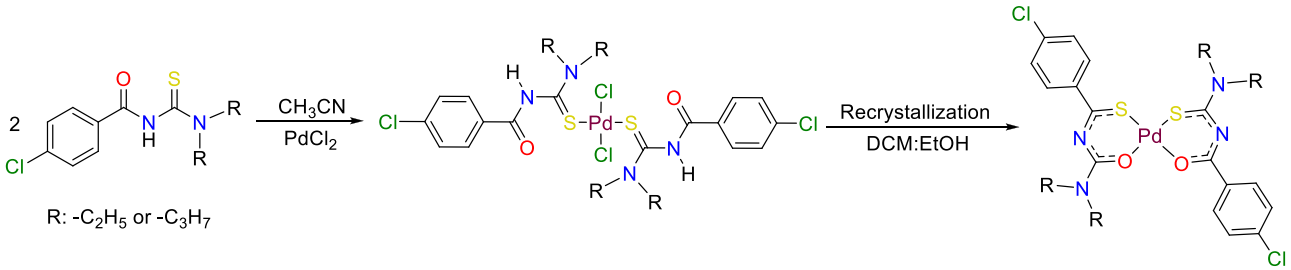

SCHEME 2 Synthesis of the palladium complexes

ν(C=O) 1680 (s); ν(C=S) 1258 (s); ν(C–Cl) 750 (s). ^{1}H NMR (400 MHz, $CDCl_3$, δ, ppm): 11.41 (s, 1H, NH), 10.98 (s, 1H, NH), 8.06 (d, $J = 8.2$ Hz, 2H, Ar–H), 7.96 (d, $J = 8.4$ Hz, 2H, Ar–H), 7.43 (d, $J = 8.1$ Hz, 4H, Ar–H), 3.96 (q, $J = 7.1$ Hz, 4H, CH_2), 3.55 (q, $J = 7.2$ Hz, 4H, CH_2), 1.43 (t, $J = 7.2$ Hz, 6H, CH_3), 1.31 (t, $J = 7.2$ Hz, 6H, CH_3). ^{13}C NMR (100 MHz, $CDCl_3$, δ, ppm): 177.6 (2C, C=S), 162.4 (2C, C=O), 140.2, 130.3, 129.3 (12C, C–Ar), 49.9, 48.2 (4C, C–N), 12.7, 11.8 (4C, CH_3). Anal. calcd. for $C_{24}H_{30}Cl_4N_4O_2PdS_2$: C, 40.10; H, 4.21; N, 7.80. Found: C, 40.50; H, 4.20; N, 7.80%.

2.3.2 | Synthesis of dichloro *bis*[4-chloro-*N*-(di-*n*-propylcarbamothioyl)benzamido-κS] palladium(II) [$PdCl_2(HL^2$-κS$)_2$]

4-Chloro-*N*-(di-*n*-propylcarbamothioyl)benzamide (HL^2) (1.1×10^{-2} mol) dissolved in acetonitrile were added dropwise to an acetonitrile solution of $PdCl_2$ (5×10^{-3} mol) at room temperature. The resulting mixture was stirred overnight. The orange powder that formed was filtered and washed with diethyl ether and then dried in vacuum[59] (Scheme 2).

Color: Orange. Yield: 82%. FT-IR (ATR, ν, cm^{-1}): ν (NH) 3077 (w); ν (ArH) 3020 (w); ν (CH) 2966, 2931, 2877 (w); ν(C=O) 1694 (s); ν(C–N) 1593 (w); ν(C=S) 1212 (s); ν(C–Cl) 747 (s). ^{1}H NMR (400 MHz, $CDCl_3$, δ, ppm): 11.40 (s, 1H, NH), 11.04 (s, 1H, NH), 8.02 (d, $J = 8.4$ Hz, 4H, Ar–H), 7.43 (dt, $J = 13.7$, 2.0 Hz, 4H, Ar–H), 3.86 (td, $J = 15.2$ Hz, 4H, N–CH_2), 3.43 (td, $J = 8.1$, 7.3 Hz, 4H, N–CH_2), 1.89 (h, $J = 7.4$ Hz, 4H, CH_2), 1.69 (h, $J = 7.5$ Hz, 4H, CH_2), 1.06 (t, $J = 7.4$ Hz, 6H, CH_3), 0.86 (t, $J = 7.4$ Hz, 6H, CH_3). ^{13}C NMR (100 MHz, $CDCl_3$, δ, ppm): 178.2 (2C, C=S), 162.0 (2C, C=O), 140.0, 130.2, 129.3 (12C, C–Ar), 57.0, 55.2 (4C, C–N), 21.1, 20.1 (4C, CH_2), 11.2 (4C, CH_3). Anal. calcd. for $C_{28}H_{38}Cl_4N_4O_2PdS_2$: C, 43.40; H, 4.94; N, 7.20. Found: C, 43.60; H, 4.90; N, 7.30%.

2.3.3 | *Bis*[4-chloro-*N*-(diethylcarbamothioyl)benzamido-κ^{2}O,S] palladium(II), [$Pd(L^1$-κ^{2}S,O$)_2$]

[$Pd(L^1$-κ^{2}O,S$)_2$] was obtained by recrystallization of [$PdCl_2(HL^1$-κS$)_2$] from dichloromethane/ethanol mixture (1:2, *v*:*v*) or hot acetonitrile (Scheme 2). Color: Yellow. FT-IR (ATR, ν, cm^{-1}): ν(C–H) 2973, 2929, 2864 (w); ν(C–N) 1583 (w); ν(C–O) 1485 (s); ν(C–S) 1076 (s); ν(C–Cl) 750 (s). ^{1}H NMR (400 MHz, $CDCl_3$, δ, ppm): 8.15 (dt, $J = 5.0$, 2.0 Hz, 4H, Ar–H), 7.38 (dt, $J = 5.0$, 2.3, 2.3 Hz, 4H, Ar–H), 3.84 (q, $J = 7.1$ Hz, 8H, N–CH_2), 1.27 (dt, $J = 25.0$, 7.1 Hz, 12H, CH_3). ^{13}C NMR (100 MHz, $CDCl_3$, δ, ppm): 171.4 (2C, C–S), 169.7 (2C, C–O), 137.8, 135.7, 131.0, 128.2 (12C, C–Ar), 47.3, 46.2 (4C, C–N), 13.1, 13.6 (4C, CH_3). Anal. calcd. for $C_{24}H_{28}Cl_2N_4O_2PdS_2$: C, 44.63; H, 4.37; N, 8.67. Found: C, 44.51; H, 4.32; N, 8.59%.

2.3.4 | *Bis*[4-chloro-*N*-(di-*n*-propylcarbamothioyl)benzamido-κ^{2}O,S] palladium(II), [$Pd(L^2$-κ^{2}S,O$)_2$]

[$Pd(L^2$-κ^{2}O,S$)_2$] was obtained by recrystallization of [$PdCl_2(HL^2$-κS$)_2$] from dichloromethane: ethanol mixture (1:2, *v*:*v*) or hot acetonitrile (Scheme 2). Color: Yellow. FT-IR (ATR, ν, cm^{-1}): ν(C–H) 2960, 2925, 2869 (w); ν(C–N) 1582 (w); ν(C-O) 1482 (s), ν(C–S) 1082 (s), ν(C–Cl) 749 (s). ^{1}H NMR (400 MHz, $CDCl_3$, δ, ppm): 8.13 (dt, $J = 5.0$, 2.5, 2.4 Hz, 4H, Ar–H), 7.38 (dt, $J = 4.7$, 2.3, 2.2 Hz, 4H, Ar–H), 3.73 (ddd, $J = 9.7$, 7.8, 5.5 Hz, 8H, N–CH_2), 1.85–1.76 (m, 4H, CH_2), 1.75–1.67 (m, 4H, CH_2), 0.99 (dt, $J = 17.6$, 7.4 Hz, 12H, CH_3). ^{13}C NMR (100 MHz, $CDCl_3$, δ, ppm): 171.9 (2C, C–S), 169.6 (2C, C–O), 137.7, 135.7, 131.0, 128.2 (12, C–Ar), 54.8, 53.6 (4C, C–N), 21.3, 20.8 (4C, CH_2), 11.4, 11.4 (4C, CH_3). Anal. calcd. for $C_{28}H_{36}Cl_2N_4O_2PdS_2$: C, 47.90; H, 5.17; N, 7.98. Found: C, 47.75; H, 5.10; N, 7.91%.

2.4 | Typical procedure for the Suzuki C–C coupling reaction

Arylbromide (1.0 mmol), phenylboronic acid (1.2 mmol), base (1.2 mmol), organic solvent H_2O (2:2, *v*:*v*), Bu_4NBr (0.02 mmol), and palladium catalyst (0.2 mol%) were mixed in a sealed tube, and the reaction mixture was stirred at 110°C for 18 h under aerobic conditions. At the end of this period, the reaction mixture was cooled, and then, dodecane was added to the mixture as an internal standard. The mixture was extracted with chloroform (20 mL) and washed with saturated ammonium chloride and brine. The organic phase was separated and dried over anhydrous sodium sulfate, and the solvent was evaporated. The crude product was chromatographed on silica gel, and the isolated biphenyl product was characterized by ^{1}H NMR and GC analyses.

3 | RESULTS AND DISCUSSION

3.1 | Synthesis of palladium(II) complexes

HL^1 and HL^2 were synthesized according to the procedures given in the literature.[55–58] [$PdCl_2(HL^1$-κS$)_2$] and

$[PdCl_2(HL^2\text{-}\kappa S)_2]$ were prepared by adding dropwise acetonitrile solutions of HL^1 and HL^2, respectively, to acetonitrile solution of $PdCl_2$. $[PdCl_2(HL^1\text{-}\kappa S)_2]$ and $[PdCl_2(HL^2\text{-}\kappa S)_2]$ were formed as orange powder. $[Pd(L^1\text{-}\kappa^2O,S)_2]$ and $[Pd(L^2\text{-}\kappa^2O,S)_2]$ were obtained yellow crystals by recrystallization of $[PdCl_2(HL^1\text{-}\kappa S)_2]$ and $[PdCl_2(HL^2\text{-}\kappa S)_2]$ from dichloromethane/ethanol mixture (1:2, *v:v*) or hot acetonitrile, respectively. When $[PdCl_2(HL^1\text{-}\kappa S)_2]$ and $[PdCl_2(HL^2\text{-}\kappa S)_2]$ were obtained as powder form, unfortunately, we could not crystallize in the same structure because these palladium complexes were completely converted to $[Pd(L^1\text{-}\kappa^2O,S)_2]$ and $[Pd(L^2\text{-}\kappa^2O,S)_2]$ structures after recrystallization.

The palladium(II) ions in $[PdCl_2(HL^1\text{-}\kappa S)_2]$ and $[PdCl_2(HL^2\text{-}\kappa S)_2]$ complexes were coordinated to the ligands as neutral monodentate coordination through the only sulfur atoms. However, in $[Pd(L^1\text{-}\kappa^2O,S)_2]$ and $[Pd(L^2\text{-}\kappa^2O,S)_2]$ complexes, palladium(II) ions were coordinated to the corresponding ligands as monoanionic bidentate coordination through the sulfur and oxygen atoms.

All new palladium(II) complexes are air stable and soluble in common organic solvent such as acetone, dichloromethane, chloroform, 1,4-dioxane, dimethyl sulfoxide, and dimethylformamide (DMF), but insoluble in *n*-hexane, ethanol, and water.

The prepared palladium(II) complexes were characterized by elemental analyses, FT-IR, ^{1}H NMR, ^{13}C NMR, and X-ray diffraction analysis. The analytical and spectroscopic data are consistent with the proposed structures given in Scheme 2.

3.2 | FT-IR and NMR spectroscopic studies

In Section 2, FT-IR spectra of the desired compounds are given to determine the most important infrared (IR) spectral bands of ligands and palladium(II) complexes. The vibration frequencies between ligands and complexes are described by comparative analyses, and the analyses of the complexes obtained in different binding modes are compared with each other (Figure 1).

In Figure 1, the FT-IR spectrum exhibited a strong stretching absorption band at 3275 cm^{-1}, which indicates the presence of N–H group in structure of ligand HL^1. Because the ligand exhibits neutral monodentate (hypodentate) coordination via the sulfur atom to the palladium(II) ion, the deprotonation did not occur in this complex. Therefore, the related N–H stretching mode was observed at 3122 and 3087 cm^{-1} in $[PdCl_2(HL^1\text{-}\kappa S)_2]$ and $[PdCl_2(HL^1\text{-}\kappa S)_2]$ complexes, respectively. Although $[PdCl_2(HL^1\text{-}\kappa S)_2]$ complex converted to $[Pd(L^1\text{-}\kappa^2O,S)_2]$ complex during the crystallization, it has been seen that deprotonation of amidic protons (C(O)–N*H*–C(S) moiety) occured; hence, the ligand coordinated to the palladium(II) center via the sulfur and oxygen atoms in monoanionic bidentate form. The presence of C=O groups in HL^1 and $[PdCl_2(HL^1\text{-}\kappa S)_2]$ was determined with the observation of a strong absorption band at 1675 and 1680 cm^{-1}, respectively. Absorption bands belonging to C=S moiety in HL^1 and $[PdCl_2(HL^1\text{-}\kappa S)_2]$ compounds were observed as medium intensity bands at 1281 and 1258 cm^{-1} in the FT-IR spectrum. This situation

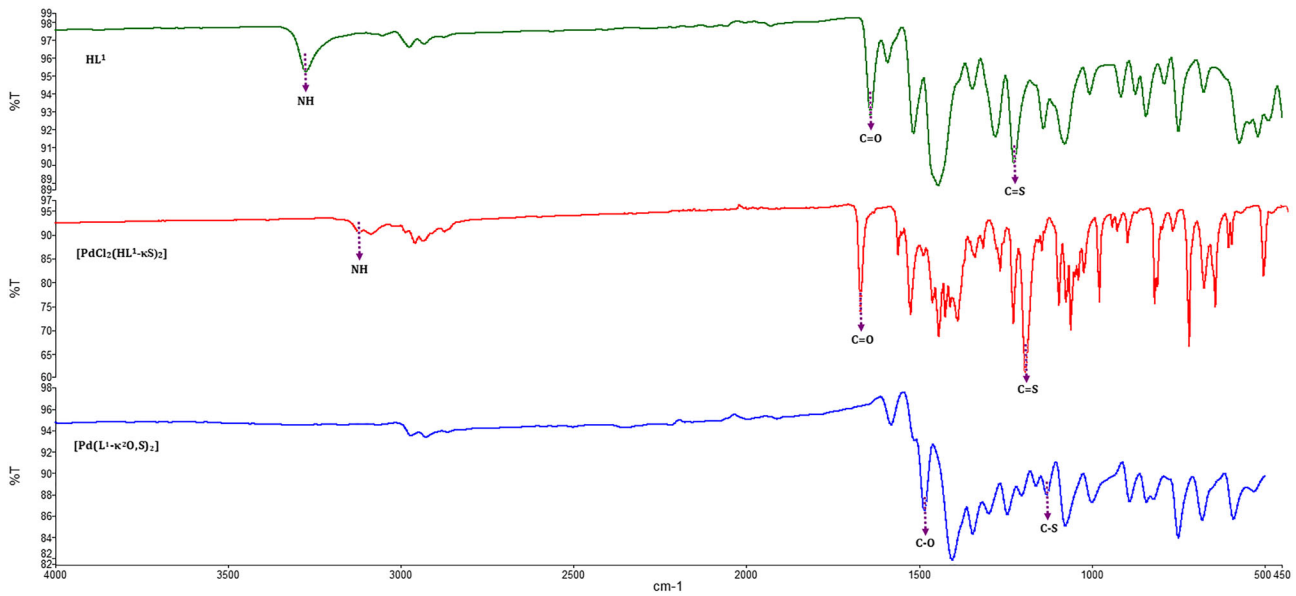

FIGURE 1 The comparison FT-IR spectra of HL^1, $[PdCl_2(HL^1\text{-}\kappa S)_2]$, and $[Pd(L^1\text{-}\kappa^2O,S)_2]$ compounds

indicates that the carbonyl moiety is in a similar environment with the ligand and its complex, and thus, it was free from coordination. But the band belonging to the C=S group appeared in the lower frequency region in the IR spectrum of the $[PdCl_2(HL^1\text{-}\kappa S)_2]$ complex; thus, it was observed that the sulfur atom of the thiocarbonyl group is involved in coordination. C=S and C=O stretching modes observed in HL^1 and $[PdCl_2(HL^1\text{-}\kappa S)_2]$ compounds disappeared in the $[Pd(L^1\text{-}\kappa^2O,S)_2]$ complex, and new ν(C–O) and ν(C–S) streching modes were observed in 1485 and 1076 cm^{-1}, respectively.

NH vibration bands exhibited at 3276 and 3077 cm^{-1} in HL^2 and $[PdCl_2(HL^2\text{-}\kappa S)_2]$, respectively. In addition, the stretching frequencies assigned to C=O and C=S groups were appeared at 1690, 1694 cm^{-1} and 1257, 1212 cm^{-1}, respectively. In the $[Pd(L^2\text{-}\kappa^2O,S)_2]$ complex, the frequencies related to C=O and C=S groups in HL^2 and $[PdCl_2(HL^2\text{-}\kappa S)_2]$ disappeared, and new C–O and C–S stretching vibration modes at 1482 and 1082 cm^{-1} were observed. These results showed us that similar situations in Figure 1 were realized.

Molecular structures of the complexes were also examined by NMR (^1H and ^{13}C) spectroscopy, and comparative analysis on the basis of spectroscopic data of both ligands and palladium(II) complexes was examined in a similar manner to the FT-IR analysis described above. In the ^1H NMR spectra of the HL^1 and HL^2 ligands, proton signals assigned to NH group were appeared as broad signals at δ 8.27 and δ 8.29 ppm, respectively. NH proton signals of $[PdCl_2(HL^1\text{-}\kappa S)_2]$ and $[PdCl_2(HL^2\text{-}\kappa S)_2]$ complexes were observed at δ 10.98 and δ 11.40 ppm, respectively. The NH signals of the palladium(II) complexes shifted downfield from their positions compared with free ligands. This situation is due to the intramolecular hydrogen bonding between the N–H groups and the chloro atoms coordinated to palladium metal.[44] However, the NH proton signals that existed in the ligands and $[PdCl_2(HL\text{-}\kappa S)_2]$ complexes disappeared in those of $[Pd(L^1\text{-}\kappa^2O,S)_2]$ and $[Pd(L^2\text{-}\kappa^2O,S)_2]$ complexes due to the coordination of the both sulfur and oxygen donors to the palladium center. The deprotonation of the N–H group was also observed from FT-IR analysis.

In the $[Pd(L^1\text{-}\kappa^2O,S)_2]$ and $[Pd(L^2\text{-}\kappa^2O,S)_2]$ complexes, the disappearance of the N–H proton after the ligands are coordinated to the palladium metal is related to the increase in the electron density of the C–N bond in the complexes.[60-62] Therefore, a slight downfield shift was also observed in the aromatic protons of $[Pd(L^1\text{-}\kappa^2O,S)_2]$ and $[Pd(L^2\text{-}\kappa^2O,S)_2]$ complexes, compared with the chemical shift of free ligands. The aromatic protons appeared in the region δ 7.78–7.45 ppm for the ligands in the region δ 8.15–7.38 ppm for the corresponding palladium(II) complexes.

The eight proton signals corresponding to the CH_2 protons were observed as two quartets at δ 3.96 and 3.55 ppm, and the 12 proton signals assigned to the CH_3 protons were observed as again two doublets at δ 1.43 and 1.31 ppm in the ^1H NMR spectrum of $[PdCl_2(HL^1\text{-}\kappa S)_2]$. In the $[Pd(L^1\text{-}\kappa^2O,S)_2]$ complex, N–CH_2 proton signals appeared as single quartets at δ 3.84 ppm, and the signals corresponding to the CH_3 protons were observed as two triplets at δ 1.34 and 1.27 ppm. In the ^1H NMR spectrum of $[PdCl_2(HL^2\text{-}\kappa S)_2]$, two triplets at δ 3.86 and 3.43 ppm, two multiplets in the regions δ 1.93–1.84 ppm and δ 1.74–1.65 ppm, and two triplets at δ 1.06 and 0.86 ppm were observed, which were assigned to the methylene protons of N–CH_2 groups, CH_2 protons, and terminal methyl protons in the aliphatic chain, respectively.

The observation of signals at δ 179.08 and 177.55 ppm and at δ 162.82 and 162.37 ppm in the ^{13}C NMR spectra of HL^1 and $[PdCl_2(HL^1\text{-}\kappa S)_2]$ confirmed the presence of C=S and C=O groups, respectively. The signals assigned to the C–S and C–O groups in $[Pd(L^1\text{-}\kappa^2O,S)_2]$ were appeared in δ 171.40 and 166.72 ppm. In the ^{13}C NMR spectrum, C=S and C=O carbons of HL^2 and $[PdCl_2(HL^2\text{-}\kappa S)_2]$ were observed also at δ 179.76 and 178.23 ppm and δ 162.61 and 162.04 ppm, respectively. In the $[Pd(L^2\text{-}\kappa^2O,S)_2]$ complex, carbon atoms of the same groups were shown at δ 171.94 and 169.56 ppm. The cause of chemical shifts in $[Pd(L\text{-}\kappa^2O,S)_2]$ complexes relates to the neutral bidentate coordination to the palladium(II) center through the sulfur and oxygen atoms.

In both $[Pd(L\text{-}\kappa S)_2]$ complexes, signals of the thiocarbonyl carbons in corresponding ligands were shifted after each ligand coordinated to the palladium center, which indicates that coordination occured only through the sulfur atoms for the formation of neutral monodentate palladium(II) complexes. On the other hand, the signals of the other hydrogen and carbon atoms of all ligands and were appeared in the expected regions. Thus, as expected, all the results that we found support our suggested molecular and bonding structures (Sections 2.2 and 2.3).

3.3 | Crystal structure analysis

X-ray quality crystals of the prepared complexes were obtained from dichloromethane:/ethanol mixture (1:2, *v*:*v*) or hot acetonitrile (Figure 2). Block-shaped orange-colored crystals of complexes $[Pd(L^1\text{-}\kappa^2O,S)_2]$ and $[Pd(L^2\text{-}\kappa^2O,S)_2]$ crystallize in a triclinic crystal system with *P*-1 space group (Table 1). The asymmetric unit of the complex consists of one Pd(II) center with coordination

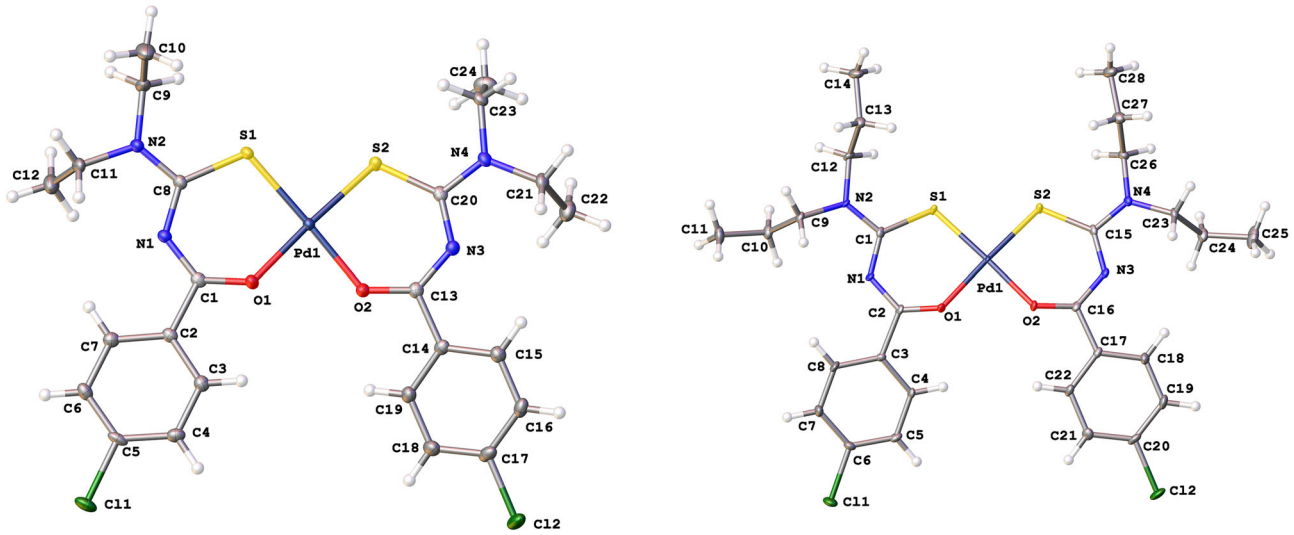

FIGURE 2 The crystal structures of the compounds $[Pd(L^1\text{-}\kappa^2O,S)_2]$ and $[Pd(L^2\text{-}\kappa^2O,S)_2]$

by two sulfur and two oxygen atoms from two mono-anionic ligand moieties (L^-). Total of angles around Pd(II) centers of the complexes $[Pd(L^1\text{-}\kappa^2O,S)_2]$ and $[Pd(L^2\text{-}\kappa^2O,S)_2]$ are 360° and 359°, indicating almost undistorted square planar geometry around the Pd(II) center, respectively. The bond lengths and bite angles are very similar to those observed for other Pd(II) complexes.[63] The chelate bite angles (°) for the six-membered ring in complexes are S1–Pd1–O1 = 93.87(4) and S2–Pd1–O2 = 92.67(4)° for complex $[Pd(L^1\text{-}\kappa^2O,S)_2]$ and S1–Pd1–O1 = 93.99(5) and S2–Pd1–O2 = 93.88(5)° for complex $[Pd(L^2\text{-}\kappa^2O,S)_2]$ (Table 2).

Bond lengths in both complexes are similar. The C(O) and C(S) bond lengths in the complexes $[Pd(L^1\text{-}\kappa^2O,S)_2]$ and $[Pd(L^2\text{-}\kappa^2O,S)_2]$ are slightly longer (1.299(3) and 1.299 (3) Å for complex $[Pd(L^1\text{-}\kappa^2O,S)_2]$ and 1.299(3) and 1.299 (3) Å for complex $[Pd(L^2\text{-}\kappa^2O,S)_2]$, respectively) than the corresponding distance found in the free ligand due to coordination to Pd(II) (Table 2).[48,51] These bond lengths reflect a relatively extent of electron delocalization over the six-membered Pd-SCNCO chelate ring, because the corresponding thiocarbonyl and carbonyl formal double bond is substantially longer in the free ligand.[31,63,64]

On the other hand, single-crystal X-ray diffraction analysis of complexes indicates significant intra- and intermolecular interactions that appear to stabilize the solid state. Intra- and intermolecular hydrogen bonds and geometrical parameters are given in Tables 3 and 4 for complexes. In the molecular packing structure of the complex $[Pd(L^1\text{-}\kappa^2O,S)_2]$, the molecules are linked through intermolecular C–H···Cl, C–H···S interactions and π···π stacking interactions to form supramolecular structure (Figure 3). The intermolecular C–H···Cl interactions occur between the chlorine atoms and the aromatic ring hydrogen atoms, forming dimeric $R^2_2(28)$ and synthons, whereas the intermolecular C–H···S interactions occur between the thiocarbonyl sulfur atoms and the aliphatic hydrogen atoms, forming dimeric $R^2_2(14)$. The molecular structure of complex $[Pd(L^1\text{-}\kappa^2O,S)_2]$ also shows significant intermolecular π···π stacking interactions between the planar six-membered Pd-SCNCO chelate ring and the phenyl ring of the neighboring molecule. These π···π stacking interactions are face-to-face, and the average interplanar distance between these π-stacked aromatic moieties is 3.405 Å with symmetry code: $i = -x, 1\text{-}y, -z$ (Figure 3).

Examination of the packing for the complex $[PdL^2\text{-}\kappa^2O,S_2]$ showed intermolecular C–H···Cl interactions between the chlorine atom and the ethyl or aromatic ring hydrogen atom of an adjacent molecule. The C–H···Cl interactions provide contribution to the polymeric chain along the *c* axis, leading to the formation of fused dimeric $R^2_2(28)$ and tetrameric $R^4_4(30)$ synthons (Figure 4). On the other hand, unlike complex $[Pd(L^1\text{-}\kappa^2O,S)_2]$, the molecules of complex $[Pd(L^2\text{-}\kappa^2O,S)_2]$ are assembled through π-stacking interactions slightly offset relative to one another between the aromatic rings of thiourea ligands. Corresponding distances for these interactions are 3.939 Å with symmetry code $i = -1 + x, y, z$ (Figure 5). Furthermore, additional C–H···π stacking interactions occur between Pd–S–C–N–C–O chelate ring and aliphatic hydrogen atoms, and these interactions lead to the stabilization of three-dimensional supramolecular structure of the complex $[Pd(L^2\text{-}\kappa^2O,S)_2]$ (Figure 5).

TABLE 1 Crystal data and details of the structure refinement for complexes $[Pd(L^1\text{-}\kappa^2O,S)_2]$ and $[Pd(L^2\text{-}\kappa^2O,S)_2]$

Compound	$[Pd(L^1\text{-}\kappa^2O,S)_2]$	$[Pd(L^2\text{-}\kappa^2O,S)_2]$
Empirical formula	$C_{24}H_{28}Cl_2N_4O_2PdS_2$	$C_{28}H_{36}Cl_2N_4O_2PdS_2$
Formula weight	645.92	702.03
Temperature (K)	100.0	100.01
Crystal system	Triclinic	Triclinic
Space group	*P*-1	*P*-1
a (Å)	7.7253(5)	9.7269(3)
b (Å)	13.7144(9)	12.8369(4)
c (Å)	13.8434(10)	13.3640(5)
α (°)	112.837(2)	66.157(2)
β (°)	92.382(2)	87.520(2)
γ (°)	95.896(2)	84.892(2)
Volume (Å^3)	1339.24(16)	1520.15(9)
Z	2	2
ρ_{calc} (g/cm^3)	1.602	1.534
μ (mm^{-1})	1.078	8.086
F(000)	656.0	720.0
Crystal size (mm^3)	0.45 × 0.14 × 0.09	0.27 × 0.26 × 0.21
Radiation	MoKα (λ = 0.71073)	CuKα (λ = 1.54178)
2Θ range for data collection (°)	5.868 to 50.224	7.232 to 133.184
Index ranges	$-9 \le h \le 9$ $-16 \le k \le 16$ $-16 \le l \le 16$	$-11 \le h \le 11$ $-15 \le k \le 15$ $-15 \le l \le 15$
Reflections collected	50,601	49,145
Independent reflections	4747 [$R_{int} = 0.0531$, $R_{sigma} = 0.0176$]	5371 [$R_{int} = 0.0994$, $R_{sigma} = 0.0370$]
Data/restraints/parameters	4747/0/321	5371/0/356
Goodness of fit on F^2	1.066	1.085
Final *R* indexes [$I \ge 2\sigma$ (I)]	$R_1 = 0.0193$, $wR_2 = 0.0471$	$R_1 = 0.0320$, $wR_2 = 0.0775$
Final *R* indexes [all data]	$R_1 = 0.0217$, $wR_2 = 0.0483$	$R_1 = 0.0339$, $wR_2 = 0.0789$
Largest diff. peak/hole (e Å^{-3})	0.34/−0.56	0.69/−1.34

3.4 | The Suzuki C–C coupling reaction

In order to evaluate the optimal reaction conditions, the effect of solvent, base, substrate to pre-catalyst ratio (S/C), and using tetrabutylammonium bromide (Bu_4NBr) as an additive were investigated on the Suzuki C–C coupling reaction between bromobenzene and phenylboronic acid in the presence of pre-catalyst $[PdCl_2(HL^2\text{-}\kappa S)_2]$. The reactions were performed with 0.2 mol% of pre-catalyst for initial tests and carried out under aerobic conditions in all cases. After screening 1,4-dioxane, DMF, toluene, and 2-propanol as solvent, in the presence of KOH, we found 11% and 44% conversion for 18 h of the reaction when using 2-propanol and toluene as solvent, respectively (Table 5, Entries 2 and 3). In DMF, good yield (67%) of coupling product was obtained after 18 h (Entry 1). Under the same conditions, the best result was obtained with 1,4-dioxane as the solvent with a good isolated yield (93%) of biphenyl (Entry 4). It seemed that polar aprotic solvents such as 1,4-dioxane and DMF played an important role in the Suzuki C–C coupling reactions as they allow for the best solubility of both the catalysts and substrates used. In addition to this, when comparing the results obtained from 1,4-dioxane and DMF, it can also be said that because the nitrogen donor in DMF is a softer base than oxygen donors in 1,4-dioxane and this solvent is more likely to coordinate to the Pd(II) center, it is more likely to interfere with catalyst activity.[65] After determining the best solvent, we also investigated the effect of the bases such as NaOAc,

TABLE 2 Selected bond lengths (Å), bond angles, and torsion angles (°) for [Pd(L^1-κ^{2}O,S)$_2$] and [Pd(L^2-κ^{2}O,S)$_2$]

Atom	Atom	Length (Å)	Atom	Atom	Atom	Angle (°)	Atom	Atom	Atom	Atom	Angle (°)
[Pd(L^1-κ^{2}O,S)$_2$]											
Pd1	S1	2.2386(5)	S1	Pd1	S2	89.075(17)	S2	Pd1	S1	C8	167.24(1)
Pd1	S2	2.2435(5)	O1	Pd1	S1	93.87(4)	O2	Pd1	S2	C20	−21.81(1)
Pd1	O1	2.0141(12)	O1	Pd1	S2	176.91(4)	O1	Pd1	S1	C8	−11.80(1)
Pd1	O2	2.0183(12)	O1	Pd1	O2	84.38(5)	S1	Pd1	S2	C20	158.36(1)
S1	C8	1.7421(18)	O2	Pd1	S1	178.24(4)	C13	O2	Pd1	S2	21.18(1)
S2	C20	1.7420(18)	O2	Pd1	S2	92.67(4)	C13	O2	Pd1	O1	−159.78(1)
O1	C1	1.267(2)	C8	S1	Pd1	107.46(6)	N1	C1	O1	Pd1	−14.36(1)
O2	C13	1.264(2)	C20	S2	Pd1	106.71(6)	C2	C1	N1	C8	178.01(1)
N1	C1	1.325(2)	C1	N1	C8	126.61(16)	O1	C1	N1	C8	−2.92(1)
N1	C8	1.343(2)	C8	N2	C9	124.35(15)	N1	C1	C2	C7	2.40(1)
N2	C8	1.338(2)	C8	N2	C11	120.46(15)	S1	C8	N1	C1	7.32(1)
N2	C9	1.461(2)	C9	N2	C11	115.20(15)	N2	C8	S1	Pd1	−176.61(1)
N2	C11	1.475(2)	C13	N3	C20	125.85(16)	S1	C8	N2	C9	3.86(1)
[Pd(L^2-κ^{2}O,S)$_2$]											
Pd1	S1	2.2431(7)	S2	Pd1	S1	87.82(2)	S2	Pd1	S1	C1	−175.16(1)
Pd1	S2	2.2407(7)	O1	Pd1	S1	93.88(5)	O1	Pd1	S1	C1	7.17(12)
Pd1	O1	2.0219(18)	O1	Pd1	S2	177.11(6)	S1	Pd1	S2	C15	177.78(1)
Pd1	O2	2.0205(18)	O2	Pd1	S1	178.09(5)	O2	Pd1	O1	C2	−164.2(2)
Cl1	C6	1.749(3)	O2	Pd1	S2	93.99(5)	Pd1	S1	C1	N1	−23.2(3)
Cl2	C20	1.749(3)	O2	Pd1	O1	84.28(7)	S1	Pd1	O1	C2	15.3(2)
S1	C1	1.743(3)	C1	S1	Pd1	107.38(9)	O2	Pd1	S2	C15	−2.82(12)
S2	C15	1.748(3)	C15	S2	Pd1	107.96(9)	S2	Pd1	O2	C16	−11.6(2)
O1	C2	1.267(3)	C2	O1	Pd1	127.55(17)	O1	Pd1	O2	C16	166.1(2)
O2	C16	1.260(3)	C16	O2	Pd1	129.16(17)	Pd1	S1	C1	N2	162.49(1)
N1	C1	1.350(4)	C2	N1	C1	125.0(2)	Pd1	S2	C15	N3	13.4(3)
N1	C2	1.322(3)	C1	N2	C9	121.5(2)	Pd1	S2	C15	N4	−168.69(1)
N2	C1	1.341(3)	C1	N2	C12	123.4(2)	Pd1	O2	C16	N3	20.7(4)
N2	C9	1.481(3)	C12	N2	C9	115.0(2)	Pd1	O2	C16	C17	−159.35(1)
N2	C12	1.465(3)	N2	C1	S1	116.0(2)	C2	N1	C1	S1	16.6(4)

TABLE 3 Intra- and intermolecular hydrogen bonds for complexes [Pd(L^1-κ^{2}O,S)$_2$] and [Pd(L^2-κ^{2}O,S)$_2$] (Å,°)[a]

Compound	D-H···A	d(D-H)	d(H···A)	d(D···A)	∠ (D-H···A)
[Pd(L^1-κ^{2}O,S)$_2$]	C(7)-H(7)···N(1)	0.95	2.46	2.7772(2)	100
	C(9)-H(9A)···S(2) ^{i}	0.99	2.85	3.6685(3)	141
	C(9)-H(9B)···S(1)	0.99	2.49	2.9467(2)	108
	C(23)-H(23B)···S(2)	0.99	2.51	2.9286(2)	105
[Pd(L^2-κ^{2}O,S)$_2$]	C(12)-H(12)···S(1)	0.99	2.51	2.936(3)	106
	C(26)-H(26A)···S(2)	0.99	2.46	2.931(3)	109

[a]Symmetry codes for co-crystal: i = 1-x, 1-y, 1-z.

K_2CO_3, Cs_2CO_3, and Et_3N, but we could not obtain a significant beneficial effect on the pre-catalyst performance (Entries 5–8). These results support that strong bases are more effective to neutralize the hydrogen halide and to generate the catalytically active species for facilities the transmetallation step in Suzuki C–C coupling

TABLE 4 Geometrical parameters of C–H···π interactions for complexes $[Pd(L^1\text{-}\kappa^2O,S)_2]$ and $[Pd(L^2\text{-}\kappa^2O,S)_2]$ (Å,°)[a]

C-H···Cg(J)[b]	H···Cg	H-perp[c]	∠C-H···Cg	γ[d]	C···Cg[e]
$[Pd(L^1\text{-}\kappa^2O,S)_2]$					
C23-H23A···Cg(1)	2.76	2.68	115	13.86	3.3030(2)
$[Pd(L^2\text{-}\kappa^2O,S)_2]$					
C10-H10B···Cg(2)	2.81	−2.79	118	6.10	3.383(3)
C24-H24A···Cg(2)	2.83	2.82	127	5.95	3.516(4)

Note: Cg(1) is the centroids of the rings Pd1-S1-C8-N1-C1-O1, and Cg(2) is the centroids of the rings Pd1-S2-C15-N3-C16-O2.

[a]Symmetry codes: $i = 1 + x, y, z$; for complex $[Pd(L^1\text{-}\kappa^2O,S)_2]$; $ii = -1 + x, y, z$ and $iii = 2\text{-}x, 1\text{-}y, 1\text{-}z$.

[b]Center of gravity of ring J (plane number above).

[c]Perpendicular distance of H to the ring plane J.

[d]Angle between Cg-H vector and the ring J normal.

[e]Distance between C atom and the nearest carbon atom in the benzene ring.

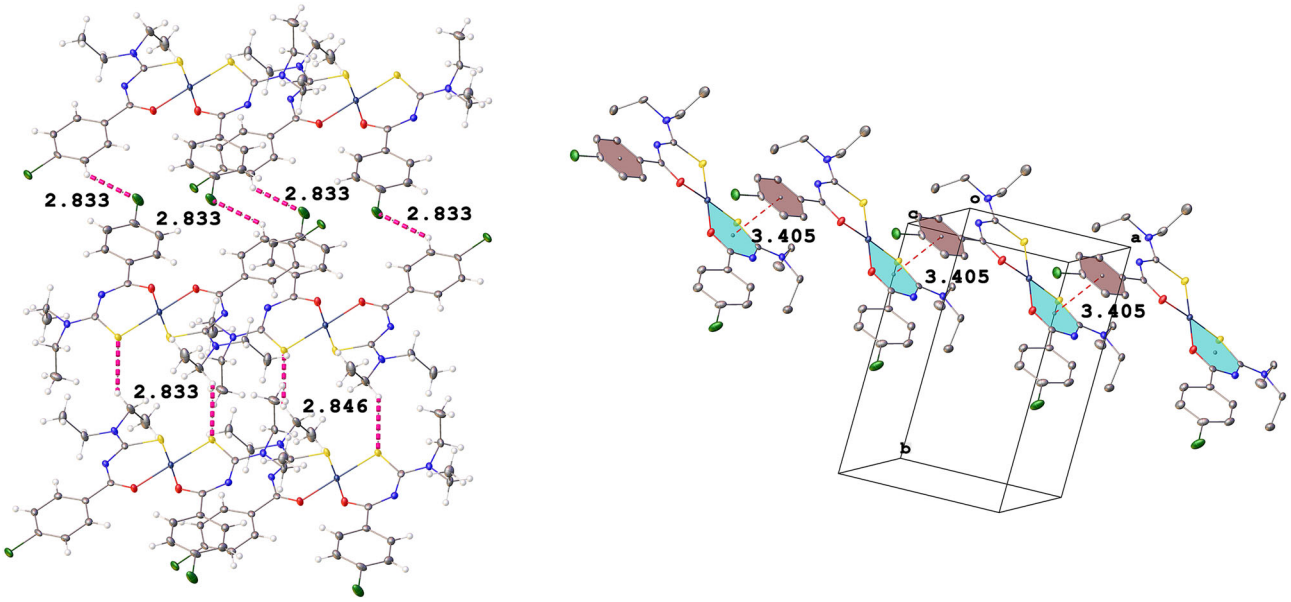

FIGURE 3 C–H···Cl intramolecular interactions and π···π stacking interactions in $[Pd(L^1\text{-}\kappa^2O,S)_2]$ complex

reaction.[66] Thus, the best solvent and the best base were found to be 1,4-dioxane and KOH, respectively. Then, we used these conditions to evaluate the effect of tetrabutylammonium bromide (Bu_4NBr) as an additive. It is well known that quaternary ammonium salts show a beneficial effect on the coupling of arylhalides with phenylboronic acids.[67] Entry 9 showed that the coupling of bromobenzene with phenylboronic acid gave a full biphenyl product (with TON 500) when 10 mol% Bu_4NBr is added to the reaction mixture.

To extend the catalytic tests of the pre-catalyst $[PdCl_2(HL^2\text{-}\kappa S)_2]$, the effect of the catalyst amount for the coupling of bromobenzene with phenylboronic acid was also studied by varying the pre-catalyst loading from 0.2 to 0.001 mol% under optimized conditions. We found that the reduction of the catalyst loading from 0.20 to 0.01 mol% led in the reaction of bromobenzene with phenylboronic acid to a product yield of >99% with TON >9900 but further decreasing the catalyst loading from 0.01 to 0.001 mol% led to a decrease in the catalytic activity (54%) (compare Entries 10 and 11, Table 5). These excellent catalytic activities showed that even using very low pre-catalyst loading conditions was capable of effectively catalyzing the coupling of bromobenzene and phenylboronic acid at 110°C. Thus, the optimized reaction conditions are summarized as follows: 0.01 mol% of catalyst, 110°C, KOH in 1,4-dioxane.

The catalytic activities of $[PdCl_2(HL^1\text{-}\kappa S)_2]$, $[Pd(L^1\text{-}\kappa^2S,O)_2]$, and $[Pd(L^2\text{-}\kappa^2S,O)_2]$ were also investigated following identical optimized reaction conditions for the model coupling reaction, and excellent yield and selectivity were obtained over the same period (Table 6, Entries 1, 3, and 7).

At this stage, Hg(0) poisoning tests were performed for all pre-catalysts to understand whether the catalytically active species is the molecular benzoylthiourea-

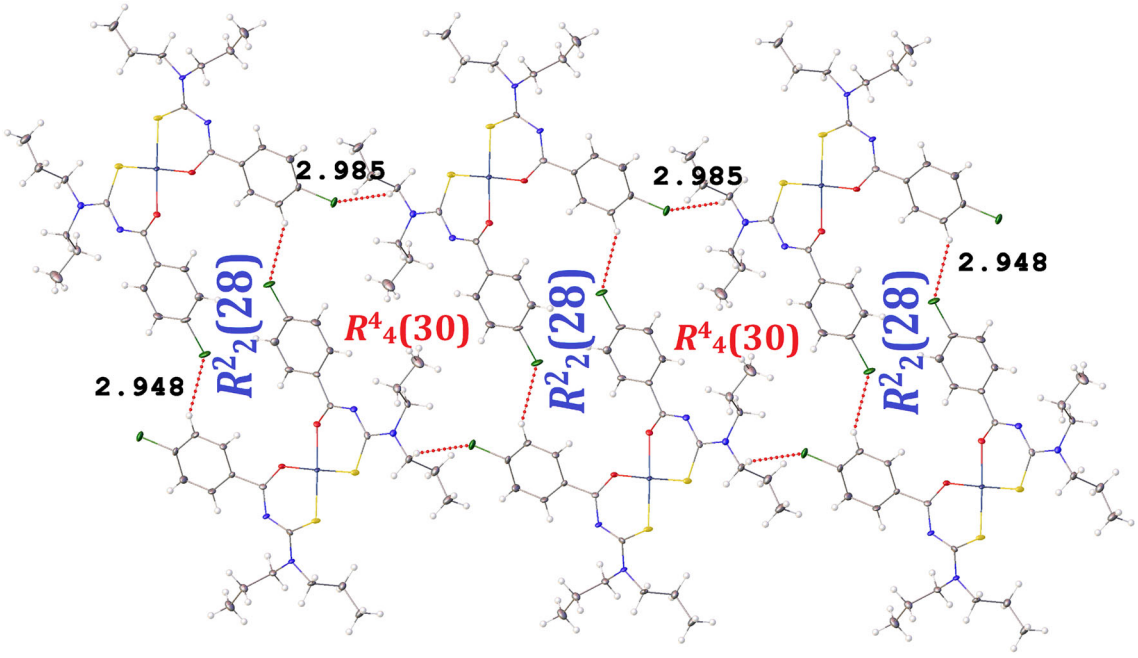

FIGURE 4 Consecutive the formation dimeric $R^2_2(28)$ and tetrameric $R^4_4(30)$ synthons generated through C–H···Cl intermolecular interactions

palladium(II) complex or nanoparticles (colloidal species or other Pd(0) particles) due to the formation of the black colloidal precipitates in all runs. It is known that the Hg(0) poisoning test is the most widely used and simple test of homogeneous versus heterogeneous catalysis. If the catalytic reaction were supported with palladium (0) species such as nanoclusters or colloidal palladium(0), the catalyst activity would be dramatically decreased by the Hg(0) addition. It was observed that addition of 20 equivalents Hg(0) at the beginning of the reaction completely suppressed the catalytic activity for all of the pre-catalysts (Table 6, Entries 2, 4, 6 and 8). Despite that the only Hg(0) poisoning test has been used to assess the homogeneity or heterogeneity of our catalyst system, obtained results strongly suggest that the heterogeneously active Pd(0) species play an important role and the possibility of a homogeneous pathway cannot be presumed. These results also indicate that our thiourea ligands are highly capable of stabilizing the active catalyst; in other words, synthesized benzoylthiourea-palladium complexes are necessary intermediates for the formation of active Pd(0) species in the reaction medium.[65,68,69] After determining the catalytic pathway, the reusability of black precipitates that produced by pre-catalyst $[PdCl_2(HL^2\text{-}\kappa S)_2]$ during the reaction under the optimized conditions was studied. At the end of each reaction, the resulting black precipitates were recovered by centrifugation and washed with chloroform, methanol, and water, respectively. Then, recovered precipitates were dried under high vacuum and used with fresh bromobenzene and phenylboronic acid. The results showed that the active catalyst could be reused for four consecutive cycles without significant loss of catalytic activity. It is worth nothing that the morphological characterization of the recovered precipitates after four successive runs was performed using TEM image analysis and the average diameter of the nanoparticles is in the range 3.6 ± 0.1 nm without obvious aggregation (see Supporting Information).

With our optimized conditions in hand, we examined a range of substituted arylhalides in the Suzuki C–C coupling reaction with phenylboronic acid. The results are summarized in Table 7. We have discovered that catalyst systems can serve as an effective catalyst considering this process for activated, sterically hindered, and deactivated arylbromides. For example, the reaction of 4-bromobenzaldehyde containing electron-withdrawing group at *para* position, which could accelerate the rate-determining oxidative addition step in the catalytic cycle due to the reduced electron density of C–Br bond, gave biphenyl-4-carboxaldehyde as the principal product in excellent yields with all catalysts (Entry 3).[65,70] Our pre-catalysts are also effective toward the coupling of 2-bromobenzaldehyde, 2-bromoanisole, and 1-bromo-2-nitrobenzene, which have sterically bulky -formyl, -methoxy, and -nitro groups at the *ortho*

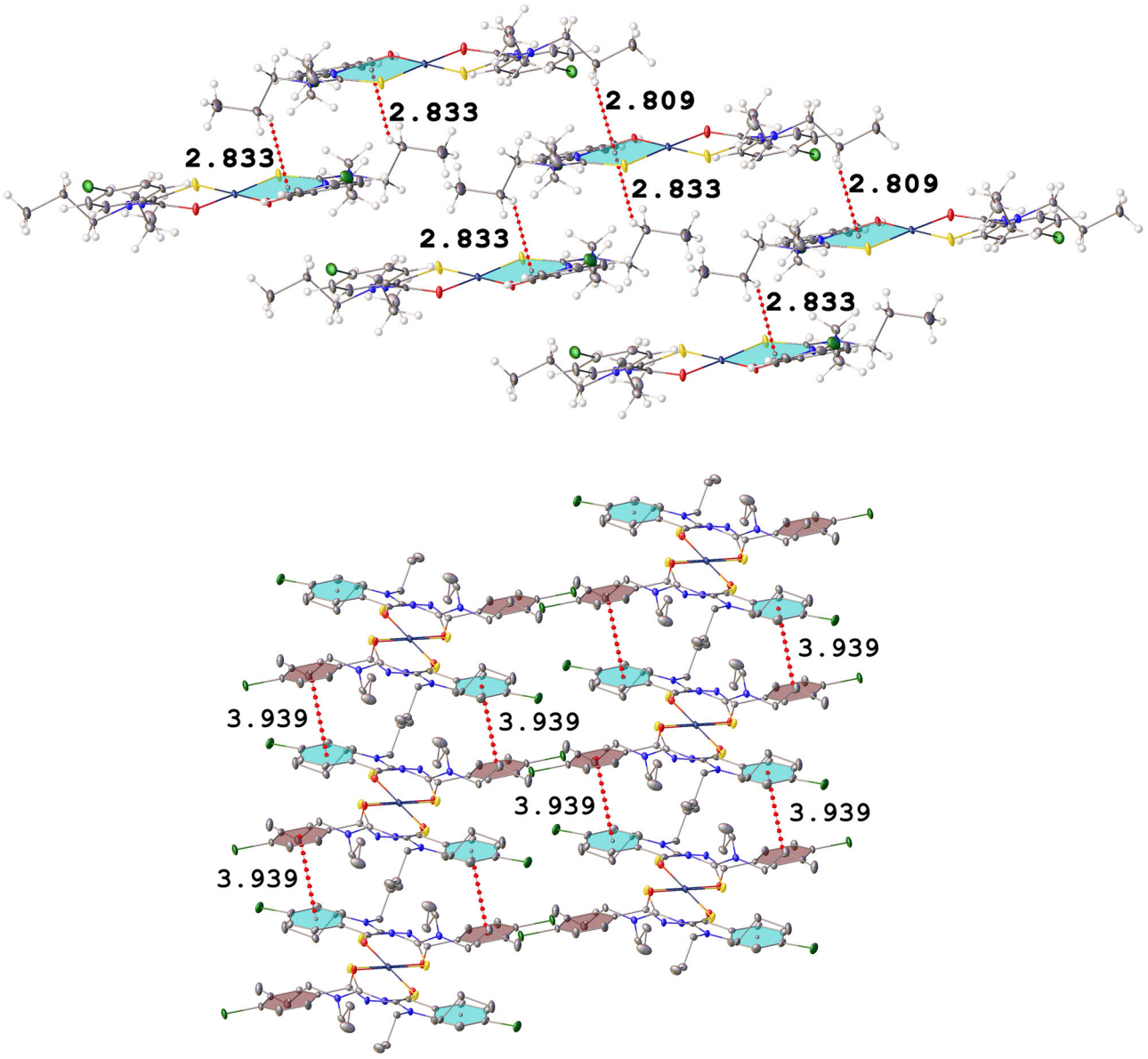

FIGURE 5 C–H···π and π···π stacking interactions in $[Pd(L^2\text{-}\kappa^2O,S)_2]$ complex

position (Entries 2, 7, and 8). In spite of this steric hindrance, $[Pd(L^1\text{-}\kappa^2S,O)_2]$ gave biphenyl-2-carboxaldehyde as the major product with >99% conversion and 87% selectivity, whereas other complexes gave the conversion in the range of 74%–84%, and thus, steric effect was well tolerated. Generally, for the Suzuki C–C coupling reactions, the use of deactivated arylbromides, substituted with electron-donating groups such as -methyl, -naphthyl, or -methoxy, reduce the rate of the reaction (Entries 9–11).[19,71] However, the coupling of 4-bromoanisole and phenylboronic acid gave desired coupled product with good to excellent isolated yields by all pre-catalysts (up to 96%), achieving a TON of 9900 (Entry 1). The catalytic activities of all palladium(II) complexes were also tested in the Suzuki C–C coupling of 1-chloro-4-nitrobenzene and heteroaromatic substrate 2-bromopyridine with phenylboronic acid, and then, moderate to good coupling products were obtained (12%–77%; Entries 4 and 12).

These results clearly indicate that Suzuki C–C coupling reactions can catalyze with excellent conversion and selectivity using the benzoylthiourea-based palladium precursors even at very low catalyst loadings. Thus, this type of molecular structures bearing benzoylthiourea-palladium complexes as pre-catalyst can be further developed in Suzuki C–C coupling reaction by changing their electronic structure and geometry.

TABLE 5 Optimization of Suzuki C–C coupling reaction condition[a]

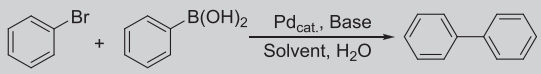

Entry	Base	Solvent	Conversion (%)[b]	Yield (%)[b]	Selectivity (%)	TON[c]
1	KOH	DMF	74	67	90	370
2	KOH	Toluene	44	44	>99	220
3	KOH	2-Propanol	11	5	45	55
4	KOH	1,4-Dioxane	93	93 (92[d])	>99	465
5	NaOAc	1,4-Dioxane	49	49	>99	245
6	Cs_2CO_3	1,4-Dioxane	13	13	>99	65
7	Et_3N	1,4-Dioxane	49	49	>99	245
8	K_2CO_3	1,4-Dioxane	6	6	>99	30
9	KOH	1,4-Dioxane	>99[e]	>99 (97[d])	>99	500
10	KOH	1,4-Dioxane	>99[e,f]	>99 (97[d])	>99	>9900
11	KOH	1,4-Dioxane	54[e,g]	54	>99	54000

[a]Reaction conditions: bromobenzene (1.0 mmol), phenylboronic acid (1.2 mmol), base (1.2 mmol), catalyst ($[PdCl_2(HL^2\text{-}\kappa S)_2]$) (0.002 mmol), solvent (2 mL), H_2O (2 mL), temperature: 110°C, time: 18 h.
[b]Yields and conversions were determined with GC analysis based on bromobenzene using dodecane as an internal standard.
[c]TON: mole product/mole catalyst.
[d]Isolated yield after silica gel chromatography.
[e]Bu_4NBr (relative to the complex used, 10%).
[f]Pre-catalyst (0.01 mol%), from the stock solution of the pre-catalyst (0.01 M).
[g]Pre-catalyst (0.001 mol%), from the stock solution of the pre-catalyst (0.01 M).

TABLE 6 Hg(0) poisoning effect on pre-catalysts for Suzuki C–C coupling reaction between bromobenzene and phenylboronic acid[a]

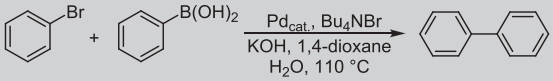

Entry	Catalyst[b]	Hg(0)[c]	Conversion (%)[d]	Yield (%)[d]	Selectivity (%)	TON[e]
1	$[PdCl_2(HL^1\text{-}\kappa S)_2]$	–	>99	>99 (96[f])	>99	9900
2		+	<1	<1	<1	–
3	$[Pd(L^1\text{-}\kappa^2 S,O)_2]$	–	>99	>99 (97[f])	>99	9900
4		+	<1	<1	<1	–
5	$[PdCl_2(HL^2\text{-}\kappa S)_2]$	–	>99	>99	>99	>9900
6		+	<1	<1	<1	–
7	$[Pd(L^2\text{-}\kappa^2 S,O)_2]$	–	>99	>99 (97[f])	>99	9900
8		+	1	1	<1	–

[a]Reaction conditions: bromobenzene (1.0 mmol), phenylboronic acid (1.2 mmol), KOH (1.2 mmol), catalyst (0.0001 mmol), Bu_4NBr (10%), 1,4-dioxane (2 mL), H_2O (2 mL), temperature: 110°C, time: 18 h.
[b]From stock solution of the catalyst (0.01 M).
[c]20 equivalent of Hg(0) (relative to the complex used) was added at the beginning of the reaction.
[d]Yields and conversions were determined by GC analysis based on bromobenzene using dodecane as an internal standard.
[e]TON: moles of product/moles of catalyst.
[f]Isolated yield after silica gel chromatography.

TABLE 7 The effect of catalysts on Suzuki C–C coupling reaction between substituted arylhalides and phenylboronic acid[a]

ArBr + PhB $(OH)_2$ → Ar–Ph

		$[PdCl_2(HL^1\text{-}\kappa S)_2]$			$[Pd(L^1\text{-}\kappa^2S,O)_2]$			$[PdCl_2(HL^2\text{-}\kappa S)_2]$			$[Pd(L^2\text{-}\kappa^2S,O)_2]$		
Entry	**ArBr**	**Conv. (%)[b]**	**Yield (%)[b]**	**TON[c]**	**Conv. (%)[b]**	**Yield (%)[b]**	**TON[c]**	**Conv. (%)[b]**	**Yield (%)[b]**	**TON[c]**	**Conv. (%)[b]**	**Yield (%)[b]**	**TON[c]**
1	4-Bromoanisole	99	90[d]	9900	87	61	8700	99	93[d]	9900	99	96[d]	9900
2	2-Bromobenzaldehyde	74	49	7400	>99	87[d]	>9900	76	44	7600	84	54	8400
3	4-Bromobenzaldehyde	>99	97[d]	>9900	>99	96[d]	>9900	>99	97[d]	>9900	>99	96[d]	>9900
4	2-Bromopyridine	37	33	3700	37	32	3700	56	48	5600	12	12	1200
5	1-Bromo-2(trifluoromethyl) benzene	38	38	3,800	47	47	4700	34	34	3400	40	40	4000
6	1-Bromo-4(trifluoromethyl) benzene	88	88	8800	90	90	9000	87	87	8700	85	85	8500
7	1-Bromo-2-nitrobenzene	>99	84	>9900	92	84	9200	>99	86	>9900	94	85	9400
8	2-Bromoanisole	72	56	7200	70	48	7000	72	50	7200	74	53	7400
9	1-Bromo-3,5-bis(trifluoromethyl) benzene	89	89	8900	85	85	8500	91	91	9100	83	83	8300
10	1-Bromonaphthalene	97	90	9700	97	94	9700	>99	96	>9900	>99	98	>9900
11	2-Bromo-6-methoxynaphthalene	95	75	9500	97	80	9700	>99	81	>9900	>99	87	>9900
12	1-Chloro-4-nitrobenzene	73	44	7300	77	43	7700	53	20	5300	64	30	6400

[a]Reaction conditions: arylhalide (1.0 mmol), phenylboronic acid (1.2 mmol), KOH (1.2 mmol), catalyst (0.0001 mmol), Bu_4NBr (10%), 1,4-dioxane (2 mL), H_2O (2 mL), temperature: 110°C, time: 18 h.
[b]Yields and conversions were determined by GC analysis based on arylhalides using dodecane as an internal standard.
[c]TON: mole product/mole catalyst.
[d]Isolated yield after silica gel chromatography.

4 | CONCLUSIONS

Both coordination modes of the palladium(II) complexes have been successfully synthesized and characterized. The molecular structure of the complexes has been confirmed by several analytical techniques and as well as X-ray crystallography of [Pd(L^1-κ^{2}S,O)$_2$] and [Pd(L^2-κ^{2}S,O)$_2$]. In addition, the catalytic activities of the synthesized palladium(II) complexes have been tested for Suzuki C–C coupling reaction. Our catalyst system is highly efficient and selective for the Suzuki C–C coupling reaction of activated, deactivated, and sterically hindered arylbromides with phenylboronic acid in reasonable reaction times (18 h), even with substrate to catalyst ratio of 10000/1. Furthermore, considering our results and the discussions above for the catalytic reactions, benzoylthiourea-palladium complexes were excellent precursors that decompose to the actual active Pd(0) species during the catalytic process.

ACKNOWLEDGMENT

This work was supported by the Mersin University Research Fund (Project No. 2018-3-AP4-3090).

CONFLICT OF INTEREST

The authors declare that they have no conflict of interest.

AUTHOR CONTRIBUTIONS

Ummuhan Solmaz: Investigation; methodology; visualization. **Ilkay Gumus:** Investigation; methodology; visualization. **Mustafa Kemal Yilmaz:** Investigation; methodology; visualization. **Simay Ince:** Investigation; methodology; visualization. **Hakan Arslan:** Formal analysis; funding acquisition; investigation; methodology; project administration; resources; supervision; visualization.

ETHICAL APPROVAL

All ethical guidelines have been adhered.

DATA AVAILABILITY STATEMENT

CCDC-1986148 ([Pd(L^1-κ^{2}S,O)$_2$]) and CCDC-1986149 ([Pd(L^2-κ^{2}S,O)$_2$]) contain the supplementary crystallographic data for this paper. These data can be obtained free of charge via https://www.ccdc.cam.ac.uk/structures/, or by emailing data_request@ccdc.cam.ac.uk, or by contacting The Cambridge Crystallographic Data Centre, 12 Union Road, Cambridge CB2 1EZ, UK; Fax: +44(0)1223-336033. Samples of the compounds are available from the author. Additional data that support the findings of this study are available in the Supporting Information.

ORCID

Ummuhan Solmaz https://orcid.org/0000-0002-3697-577X
Ilkay Gumus https://orcid.org/0000-0002-9398-0057
Mustafa Kemal Yilmaz https://orcid.org/0000-0002-9969-3956
Simay Ince https://orcid.org/0000-0002-9941-7281
Hakan Arslan https://orcid.org/0000-0003-0046-9442

REFERENCES

[1] A. Ratnam, M. Bala, R. Kumar, U. P. Singh, K. Ghosh, *J. Organomet. Chem.* **2018**, *856*, 41.
[2] R. B. Bedford, C. S. J. Cazin, D. Holder, *Coord. Chem. Rev.* **2004**, *248*, 2283.
[3] A. Fihri, P. Meunier, J. C. Hierso, *Coord. Chem. Rev.* **2007**, *251*, 2017.
[4] C. Barnard, *Platinum Met. Rev.* **2008**, *52*, 38.
[5] V. Polshettiwar, C. Len, A. Fihri, *Coord. Chem. Rev.* **2009**, *253*, 2599.
[6] A. Molnar, *Chem. Rev.* **2011**, *111*, 2251.
[7] A. R. Kapdi, I. J. S. Fairlamb, *Chem. Soc. Rev.* **2014**, *43*, 4751.
[8] N. Selander, K. J. Szaba, *Chem. Rev.* **2011**, *111*, 2048.
[9] S. M. S. Hussain, M. B. Ibrahim, A. Fazal, R. Suleiman, M. Fettouhi, B. E. Ali, *Polyhedron* **2014**, *70*, 39.
[10] Y. Ding, M. A. Clark, *ACS Comb. Sci.* **2015**, *17*, 1.
[11] Y. Ding, J. L. DeLorey, M. A. Clark, *Bioconjugate Chem.* **2016**, *27*, 2597.
[12] D. Zhang, Q. Wang, *Coord. Chem. Rev.* **2015**, *286*, 1.
[13] P. Ryberg, *Org. Process Res. Dev.* **2008**, *12*, 540.
[14] S. Rizzo, H. Waldmann, *Chem. Rev.* **2014**, *114*, 4621.
[15] J. L. Pratihar, P. Mandal, C. H. Lin, C. K. Lai, D. Mal, *Polyhedron* **2017**, *135*, 224.
[16] A. Khazaei, M. Khazaei, M. Nasrollahzadeh, *Tetrahedron* **2017**, *73*, 5624.
[17] M. K. Yılmaz, S. İnce, S. Yılmaz, M. Keleş, *Inorg. Chim. Acta* **2018**, *482*, 252.
[18] M. K. Yılmaz, *J. Supercrit. Fluids* **2018**, *138*, 221.
[19] M. K. Yılmaz, B. Guzel, *Appl. Organometal. Chem.* **2014**, *28*, 529.
[20] M. O. Karataş, N. Özdemir, B. Alıcı, İ. Özdemir, *Polyhedron* **2020**, *176*, 114271.
[21] C. Xi, Y. Wu, X. Yan, *J. Organomet. Chem.* **2008**, *693*, 3842.
[22] T. Kawano, T. Shinomaru, I. Ueda, *Org. Lett.* **2002**, *4*, 2545.
[23] C. Amatore, A. Jutand, *Coord. Chem. Rev.* **1998**, *178-180*, 511.
[24] J. Zhang, G. F. Zhao, Z. Popović, Y. Yong Lu, Y. Liu, *Mater. Res. Bull.* **2010**, *45*, 1648.
[25] H. Ali, N. Cauchon, J. E. Van Lier, *Photochem. Photobiol. Sci.* **2009**, *8*, 868.
[26] X. Feng, M. Yan, T. Zhang, Y. Liu, M. Bao, *Green Chem.* **2010**, *12*, 1758.
[27] S. Priyadarshini, P. J. A. Hoseph, P. Srinivas, H. Maheswaran, M. L. Kantam, S. Bhargava, *Tetrahedron Lett.* **2011**, *52*, 1651.
[28] M. Feuerstein, H. Doucet, M. Santelli, *Tetrahedron Lett.* **2004**, *45*, 8443.
[29] K. G. Thakur, E. A. Jaseer, A. B. Naidu, G. Sekar, *Tetrahedron Lett.* **2009**, *50*, 2865.
[30] W. M. Khairul, S. L. M. Faisol, S. M. Jasman, S. K. C. Soh, M. Shamsuddin, *BCREC* **2014**, *9*(3), 241.
[31] D. Mingji, B. Liang, C. H. Wang, Z. J. You, J. Xiang, G. B. Dong, J. H. Chen, Z. Yang, *Adv. Synth. Catal.* **2004**, *346*, 1669.
[32] H. L. Li, Z. S. Wu, M. Yang, Y. X. Qi, *Catal. Lett.* **2010**, *137*, 69.
[33] M. J. Dai, C. H. Wang, G. B. Dong, J. Xiang, T. P. Luo, B. Liang, J. H. Chen, Z. Yang, *Eur. J. Org. Chem.* **2003**, *2003*, 4346.
[34] W. Chen, R. Li, B. Han, B. J. Li, Y. C. Chen, Y. Wu, L. S. Ding, D. Yang, *Eur. J. Org. Chem.* **2006**, *2006*, 1177.

[35] S. Liu, Y. Lei, Z. Yang, Y. Lan, *J. Mol. Struct.* **2014**, *1074*, 527.
[36] H. Arslan, D. Vanderveer, F. Emen, N. Kulcu, Z. Krist-New, *Cryst. St.* **2003**, *218*, 479.
[37] L. M. Zhang, H. Y. Li, H. X. Li, D. J. Young, Y. Wang, J. P. Lang, *Inorg. Chem.* **2017**, *56*, 11230.
[38] Y. R. Lin, C. C. Chiu, H. T. Chiu, D. S. Lee, T. J. Lu, *Appl. Organometal. Chem.* **2017**, 1.
[39] A. C. Tenchiu, I. Ventouri, G. Ntasi, D. Palles, G. Kokotos, D. Kovala-Demertzi, I. D. Kostas, *Inor. Chim. Acta* **2015**, *435*, 142.
[40] N. Ozpozan, T. Ozpozan, H. Arslan, N. Kulcu, *Thermochim. Acta* **1999**, *336*, 97.
[41] H. Arslan, D. S. Mansuroglu, D. VanDerveer, G. Binzet, *Spectrochim. Acta a* **2009**, *72*, 561.
[42] S. Saeed, R. Hussain, *Eur. Chem. Bull.* **2013**, *2*, 465.
[43] A. Saeed, M. F. Erben, N. Abbas, U. Florke, *J. Mol. Struct.* **2010**, *984*, 240.
[44] N. Gunasekaran, N. S. P. Bhuvanesh, R. Karvembu, *Polyhedron* **2017**, *122*, 39.
[45] C. K. Ozer, H. Arslan, D. VanDerveer, N. Kulcu, *Molecules* **2009**, *14*, 655.
[46] C. K. Ozer, H. Arslan, D. VanDerveer, G. Binzet, *J. Coord. Chem.* **2009**, *62*, 266.
[47] A. Molter, F. Mohr, *Coord. Chem. Rev.* **2010**, *254*, 19.
[48] M. M. Sheeba, M. M. Tamizh, L. J. Farrugia, A. Endo, R. Karvembu, *Organometallics* **2014**, *33*, 540.
[49] O. V. Dolomanov, L. J. Bourhis, R. J. Gildea, J. A. K. Howard, H. Puschmann, *J. Appl. Crystallogr.* **2009**, *42*, 339.
[50] L. Palatinus, G. Chapuis, *J. Appl. Crystallogr.* **2007**, *40*, 786.
[51] L. Palatinus, A. van der Lee, *J. Appl. Crystallogr.* **2008**, *41*, 975.
[52] L. Palatinus, S. J. Prathapa, S. van Smaalen, *J. Appl. Crystallogr.* **2012**, *45*, 575.
[53] G. M. Sheldrick, *Acta Cryst. C* **2015**, *71*, 3.
[54] A. L. Spek, *Acta Cryst. C* **2015**, *71*, 9.
[55] U. Solmaz, I. Gumus, G. Binzet, O. Celik, G. K. Balci, A. Dogen, H. Arslan, *J. Coord. Chem.* **2018**, *71*, 200.
[56] H. Arslan, U. Florke, N. Kulcu, E. Kayhan, *Turk. J. Chem.* **2006**, *30*, 429.
[57] N. Ozpozan, H. Arslan, T. Ozpozan, M. Merdivan, N. Kulcu, *J. Therm. Anal. Calorim.* **2000**, *61*, 955.
[58] I. Gumus, U. Solmaz, O. Celik, G. Binzet, G. K. Balci, H. Arslan, *Eur. J. Chem.* **2015**, *6*, 237.
[59] U. Solmaz, Synthesis and characterization of the thiourea derivative palladium complexes, M. Sc Thesis, Mersin University, Mersin, Turkey, **2014**.
[60] A. M. Plutin, R. Mocelo, A. Alvarez, R. Ramos, E. E. Castellano, M. R. Cominetti, A. E. Graminha, A. G. Ferreira, A. A. Batista, *J. Inorg. Biochem.* **2014**, *134*, 76.
[61] S. Ahmad, A. A. Isab, S. Ali, *Transition Met. Chem.* **2006**, *31*, 1003.
[62] S. Ahmad, *Chem. Biodiversity* **2010**, *7*, 543.
[63] N. Selvakumaran, S. Weng Ng, E. R. T. Tiekink, R. Karvembu, *Inorganica Chim. Acta* **2011**, *376*, 278.
[64] H. Arslan, U. Florke, N. Kulcu, E. Kayhan, *Turkish J. Chem.* **2006**, *30*, 429.
[65] T. Mahamo, M. M. Mogorosi, J. R. Moss, S. F. Mapolie, J. C. Slootweg, K. Lammertsma, G. S. Smith, *J. Organomet. Chem.* **2012**, *703*, 34.
[66] S. K. C. Soh, M. Shamsuddin, *J. Chem.* **2013**, *2013*, 1.
[67] K. Selvakumar, A. Zapf, M. Beller, *Org. Lett.* **2002**, *4*, 3031.
[68] D. Olsson, O. F. Wendt, *J. Organomet. Chem.* **2009**, *694*, 3112.
[69] S. Kumar, G. K. Rao, A. Kumar, M. P. Singh, F. Saleem, A. K. Singh, *RSC Adv.* **2015**, *5*, 20081.
[70] S. M. Nobre, A. L. Monteiro, *J. Mol. Catal. A: Chem.* **2009**, *313*, 65.
[71] A. Scrivanti, M. Bertoldini, U. Matteoli, V. Beghetto, S. Antonaroli, A. Marini, B. Crociani, *J. Mol. Catal. A: Chem.* **2005**, *235*, 12.

SUPPORTING INFORMATION

Additional supporting information may be found online in the Supporting Information section at the end of this article.

How to cite this article: U. Solmaz, I. Gumus, M. K. Yilmaz, S. Ince, H. Arslan, *Appl Organomet Chem* **2021**, e6348. https://doi.org/10.1002/aoc.6348